Supporting Information

Surface-Engineered $Mo_2TiC_2T_x$ MXene for Moisture-Resilient High-Performance Energy Storage

Durga Madhab Pani[1], Sandip De[1], Olivier Plantevin[2], Yashodhan Iyer[3], Brahmananda Chakraborty[4, 5]*, Shyamal Chatterjee[1]*

[1]*Department of Physics, Indian Institute of Technology Bhubaneswar, Jatni, Odisha, India – 752050*

[2]*M2 PIE-Nouvelles Technologies de l'Energie, Laboratoire de Physique des Solides - Bureau O308, Bat.510 Campus d'Orsay 91405 Orsay, France*

[3]Department of Physics, Sardar Vallabhbhai National Institute of Technology, Surat-395007, Gujarat, India

[4]High Pressure & Synchrotron Radiation Physics Division, Bhabha Atomic Research Centre, Trombay, Mumbai-400085, India

[5]Homi J Bhabha National Institute, Bhabha Atomic Research Centre, Trombay, Mumbai-400085, India

Email: shyamal@iitbbs.ac.in , brahma@barc.gov.in

1. Preparation of MXene

The reaction taking place at the time of etching can be simplified by the following equations:

$$Mo_2TiAlC_2 + 3HF \rightarrow Mo_2TiC_2 + AlF_3 + 3/2(H_2)\uparrow \quad \text{.....(1)}$$

$$Mo_2TiC_2 + 2HF/H_2O \rightarrow Mo_2TiC_2T_x \ (T_x = -F, -OH, -O) \quad \text{.....(2)}$$

Equation (1) describes the selective removal of the Al layer from the Mo_2TiAlC_2 MAX phase during HF etching, leading to the formation of Mo_2TiC_2 and AlF_3 accompanied by hydrogen evolution. The freshly exposed Mo_2TiC_2 surfaces are highly reactive and readily undergo surface functionalization in the etching environment. As represented by Equation (2), interactions with HF, water, and dissolved oxygen result in the formation of surface termination groups (–F, –OH, and –O), yielding $Mo_2TiC_2T_x$ rather than a truly bare MXene. These terminations play a critical role in governing the chemical reactivity, wettability, and electrochemical behavior of the resulting MXene. Thus, the etching process intrinsically couples MAX phase exfoliation with simultaneous surface termination, producing a chemically functionalized layered material.

2. Calculation of supercapacitance

1.1. From CV curve: The specific capacitance (C_{sp}) was calculated from electrochemical cyclic voltammetry curves by using the following equation:

$$C_{sp}(CV) = \frac{absolute\ area\ under\ the\ CV\ curve}{potential\ sweep\ rate \times 2 \times working\ potential\ window} = \frac{\int_0^{2V_0} I(V)dV}{2 \times r \times V_0}$$

where the integral part in the numerator represents the area under the CV curve, 'r' is the sweep rate, and 'V_0' is the working potential window.

1.2. From CD curve: The specific capacitance (C_{sp}) was calculated from galvanostatic charge/discharge curves by using the following equation:

$$C_{sp} = \frac{Mass\ normalised\ current}{slope\ of\ V \sim t\ curve} = \frac{\left(\frac{I}{m}\right)}{\left(\frac{\Delta V}{\Delta t}\right)}$$

where ‘I’ is the applied constant current, m is the mass of the sample deposited on the Ni foam, $\Delta V/\Delta t$ is the slope obtained from the charge-discharge curve.

2.Result:

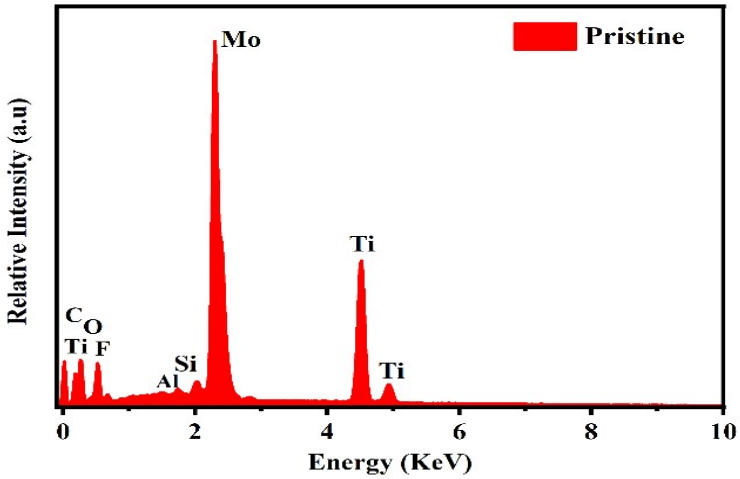

Figure S1: EDS of Pristine $Mo_2TiC_2T_x$ MXene

Table S1: Weight and Atomic percentage $Mo_2TiC_2T_x$ MXene

Elements	Weight%	Atomic%
C	34.31	59.09
O	19.52	25.24
F	3.16	3.44
Al	0.36	0.28
Ti	12.76	5.51
Mo	29.89	6.44
Total	100	100

Figure S2: EDS of $Mo_2TiC_2T_x$ irradiated MXene at a fluence of 3×10^{16} ions/cm^2

Table S2: Weight and Atomic percentage $Mo_2TiC_2T_x$ irradiated MXene at a

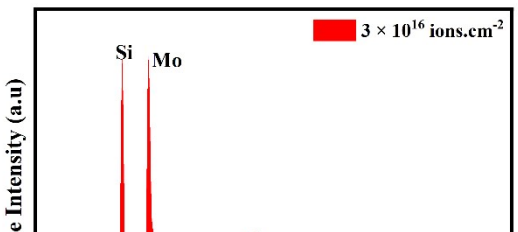

fluence of 3×10^{16} ions.cm^{-2}

Elements	Weight%	Atomic%
C	25.56	54.02
O	14.67	23.27
F	1.85	2.47
Ar	0.08	0.05
Al	0.23	0.22
Ti	17.82	9.45
Mo	39.79	10.53
Total	100	100

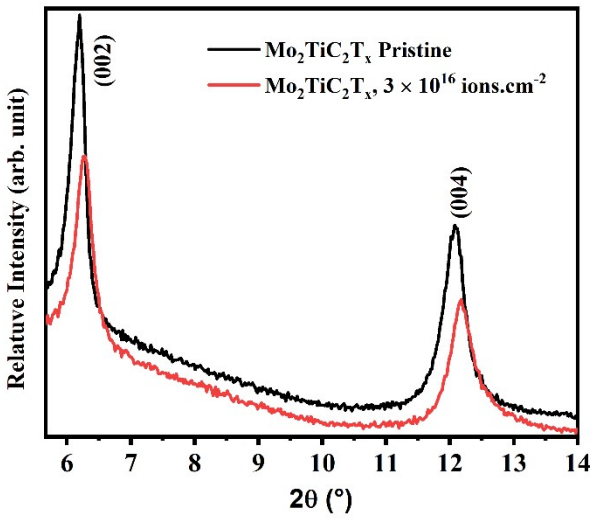

Figure S3: XRD pattern of $Mo_2TiC_2T_x$ MXene powder (black line) and irradiated MXene at an ion fluence of 3×10^{16} ions.cm^{-2} (red line) for 2θ range from 5˚ to 14˚.

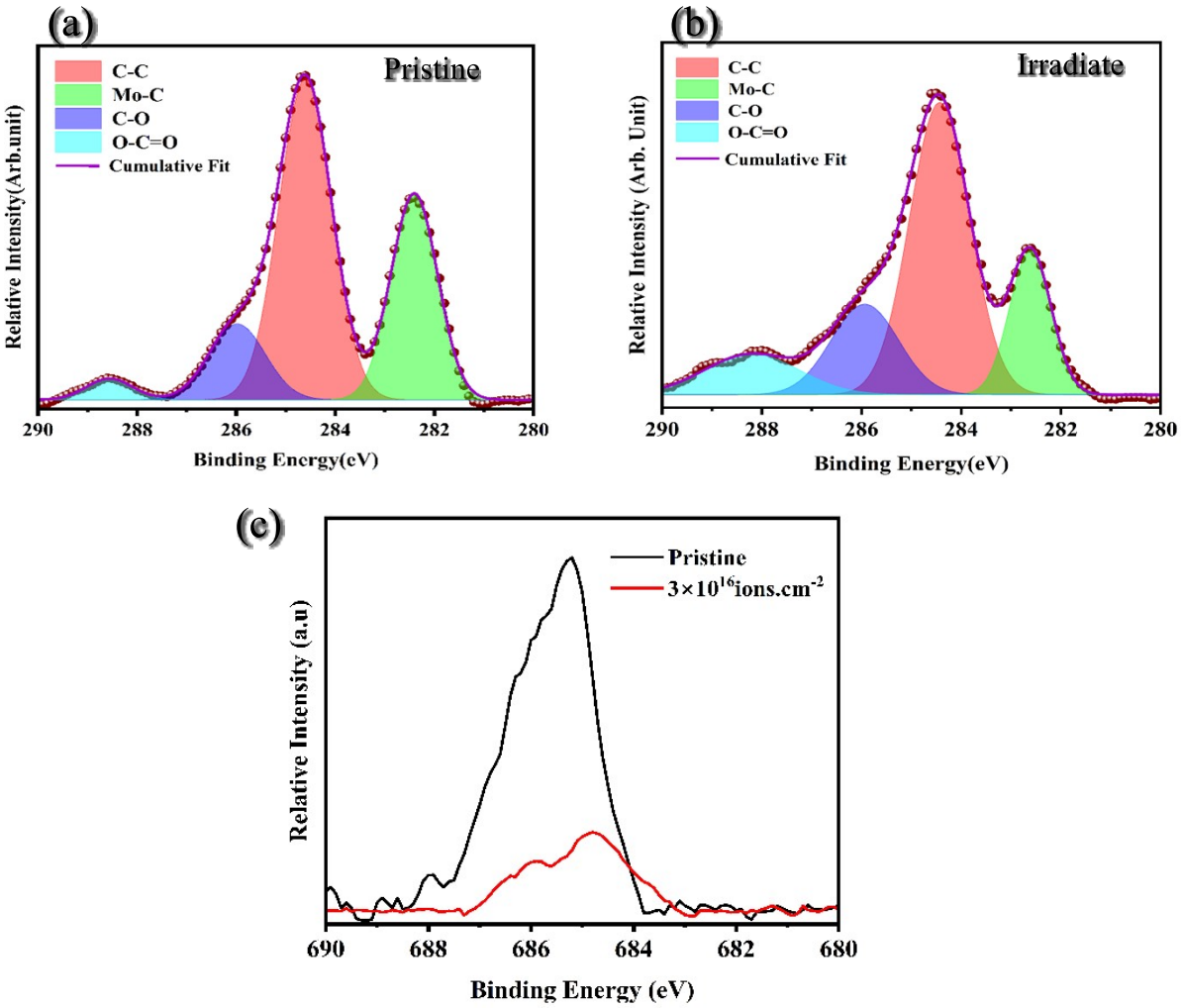

Figure S4: XPS Spectra of pristine and irradiated Mo_2TiCT_x MXene, (a-b) C 1s (c). A comparison of Fluorine spectrum in pristine and 10 keV Ar^+ ions irradiated $Mo_2TiC_2T_x$ at a fluence of 3×10^{16} ions.cm^{-2}.

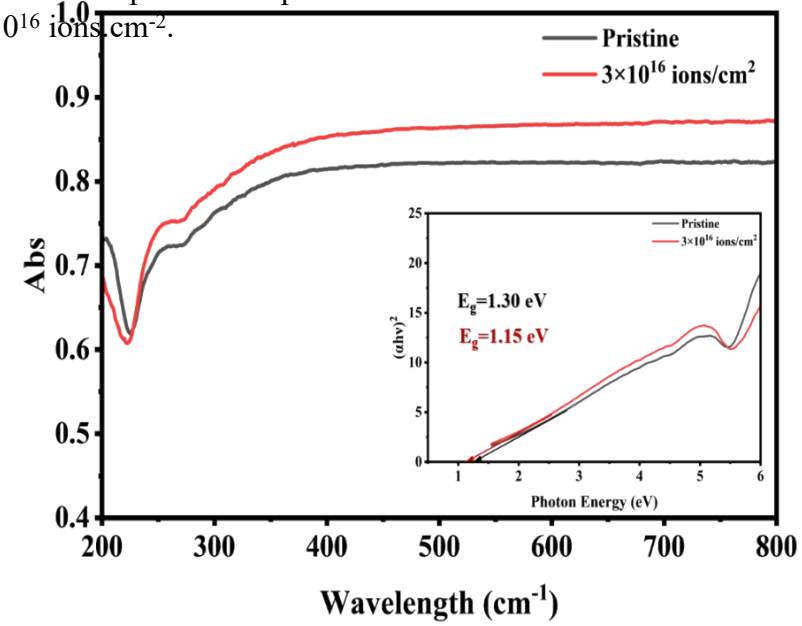

Figure S5. UV-visible absorption spectra and inset Tauc plots for both pristine and irradiated $Mo_2TiC_2T_x$ MXene

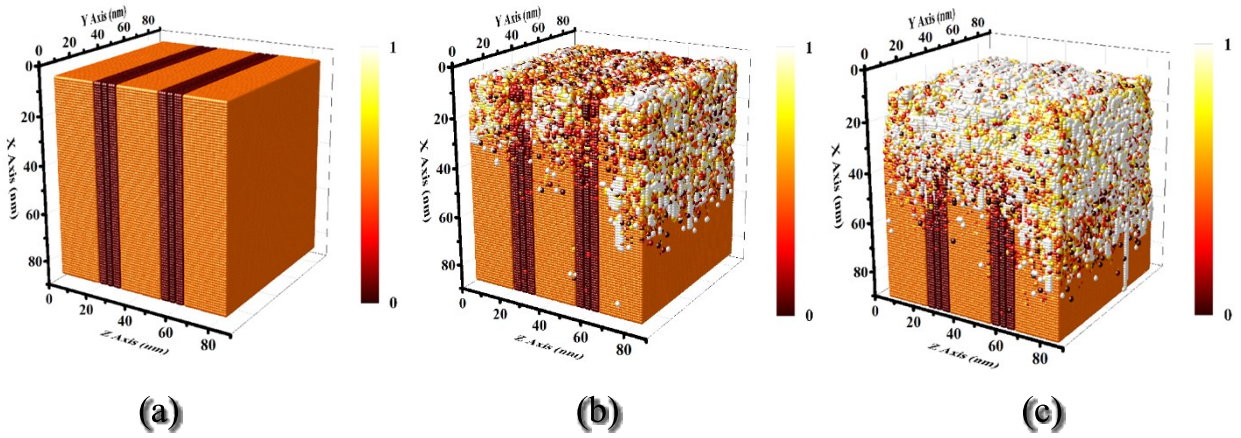

***Figure S6**: TRI3DYN Simulation result of $Mo_2TiC_2T_x$ MXene for Pristine (a) and after 10 KeV Ar^+ irradiation at ion fluence of* 1×10^{16} ions.cm^{-2}*(b) and* 3×10^{16} *ions.cm^{-2}(c).*

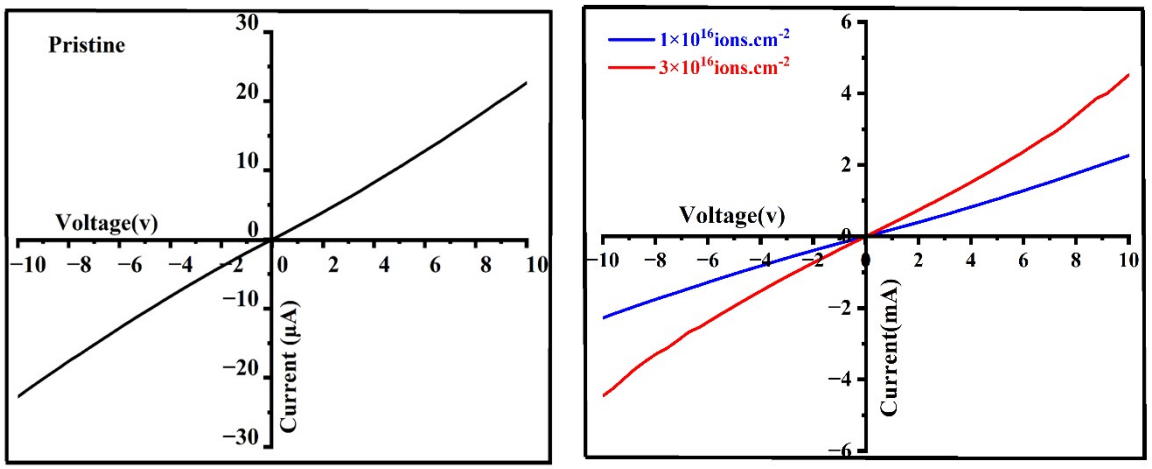

Figure S7: I-V characteristics of pristine sample (Black) and 5 KeV Ar^+ ion irradiated at two different ion fluence of 1×10^{16} ions.cm^{-2} (Blue) and 3×10^{16} ions.cm^{-2}(Red)

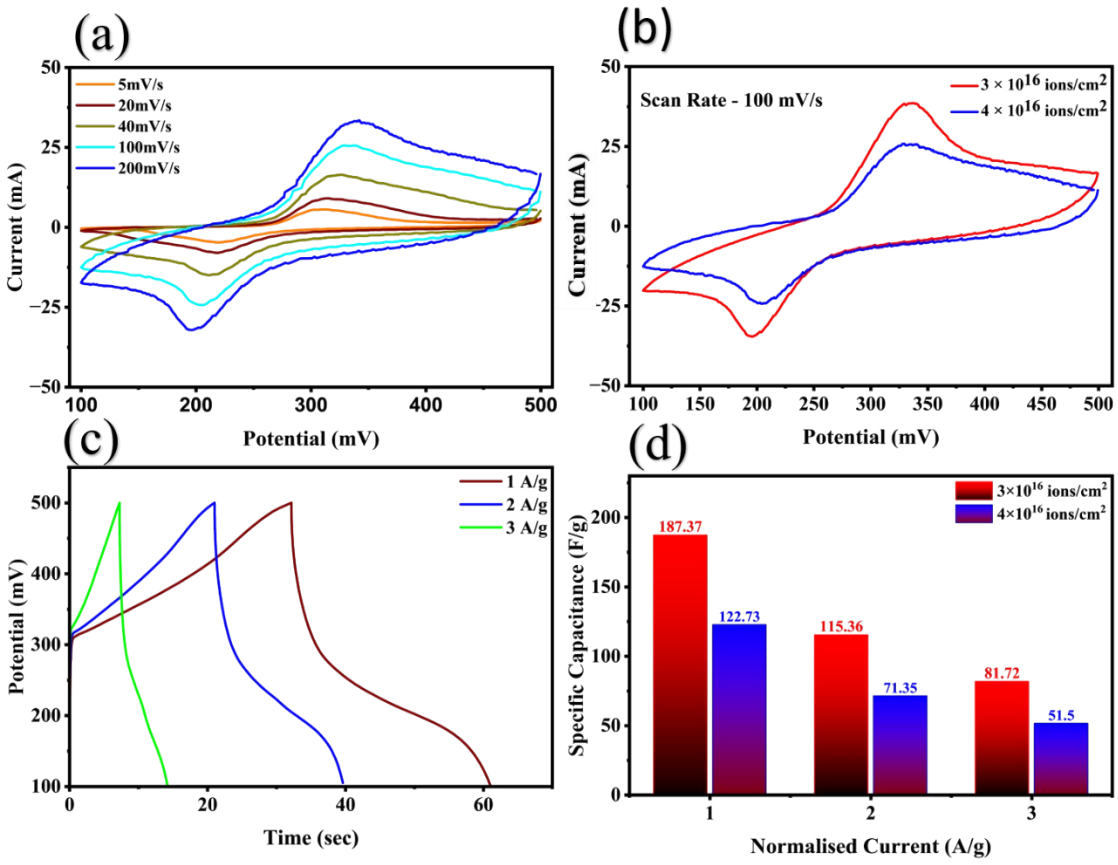

Figure S8: Cyclic voltammetry graph of ion beam modified $Mo_2TiC_2T_x$ electrode irradiated at 4 × 10^{16} ions.cm^{-2} at different scan rate (b) CV graph of ion beam modified $Mo_2TiC_2T_x$ electrode irradiated at 3 × 10^{16} ions.cm^{-2} and 4 × 10^{16} ions.cm^{-2} (scan rate= 100 mV/sec)(c) GCD graph of ion beam modified $Mo_2TiC_2T_x$ electrode irradiated at 4 × 10^{16} ions.cm^{-2} (d) Comparison of specific capacitance of ion beam modified $Mo_2TiC_2T_x$ electrode irradiated at 3 × 10^{16} ions.cm^{-2} and 4 × 10^{16} ions.cm^{-2}.

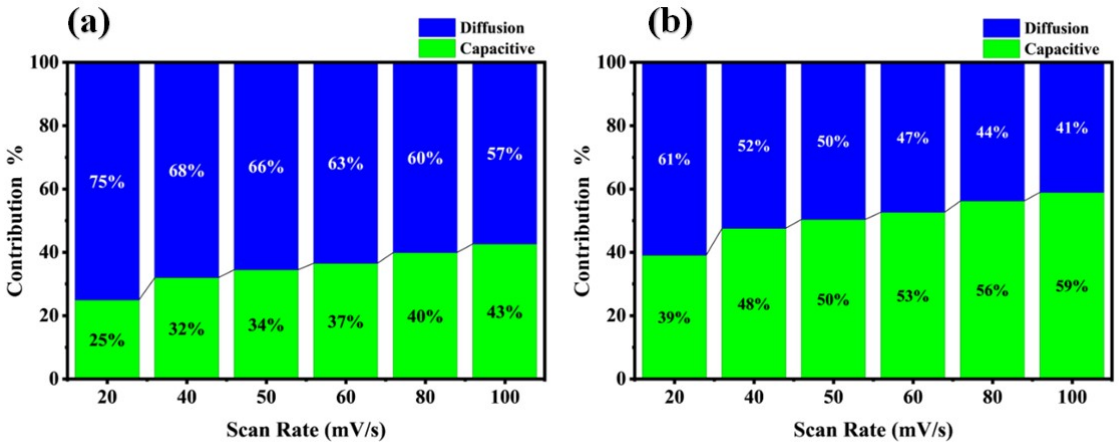

Figure S9: Capacitive and diffusive rate (%) as a function of scan rates for pristine (a) and irradiated (b) Mo_2TiC_2 MXene.

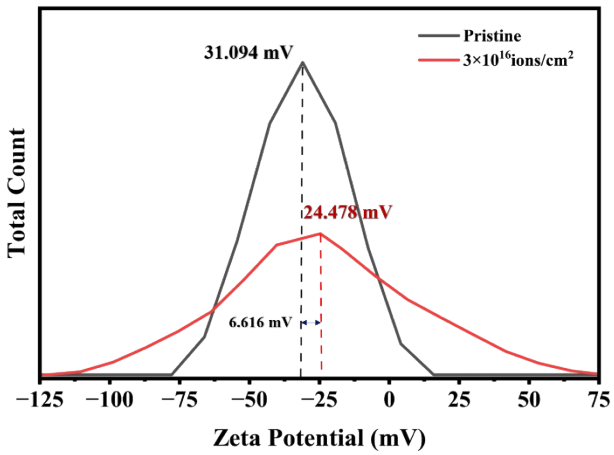

Figure S10: Comparison of Zeta potential measurements of pristine and irradiated Mo_2TiC_2 MXene.

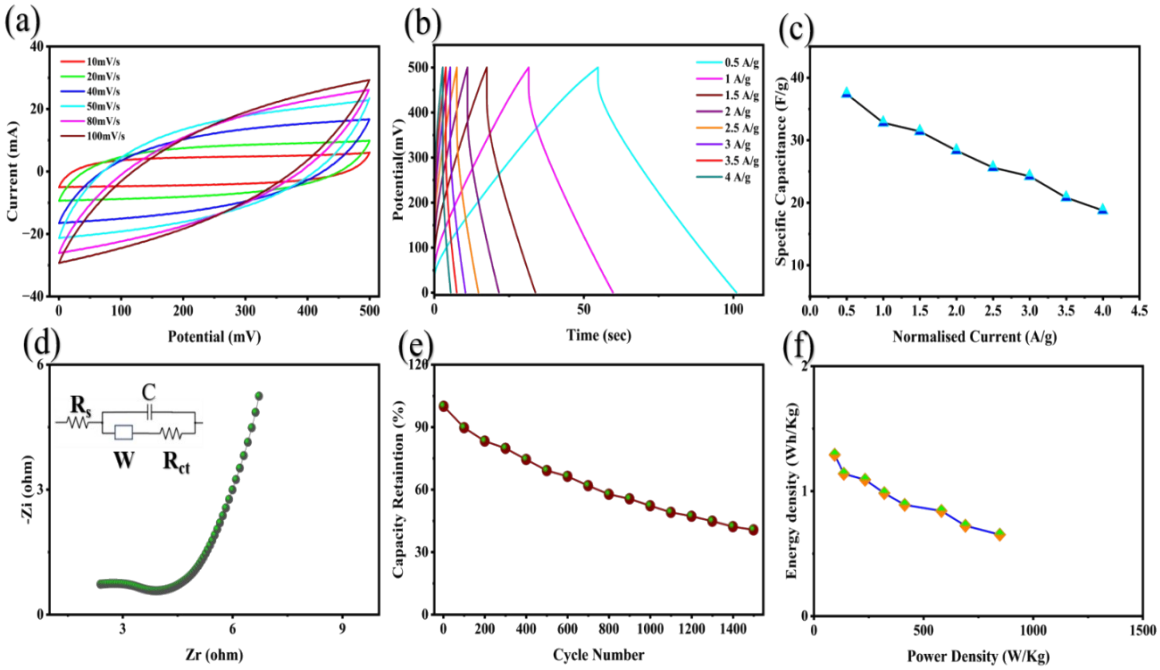

Figure S11: Electrochemical performance of the $Mo_2TiC_2T_x$ MXene-based symmetric supercapacitor device. (a) Cyclic voltammetry curves recorded at scan rates of 10–100 mV s^{-1}. (b) Galvanostatic charge–discharge profiles at current densities of 0.5–4 A g^{-1}. (c) Specific capacitance as a function of applied current density. (d) Nyquist plot recorded over a frequency range of 0.1 Hz to 100 kHz; inset shows the equivalent circuit used for impedance data fitting. (e) Capacitance retention over 1500 charge–discharge cycles at 4 A g^{-1}. (f) Ragone plot comparing the energy density and power density of the device.

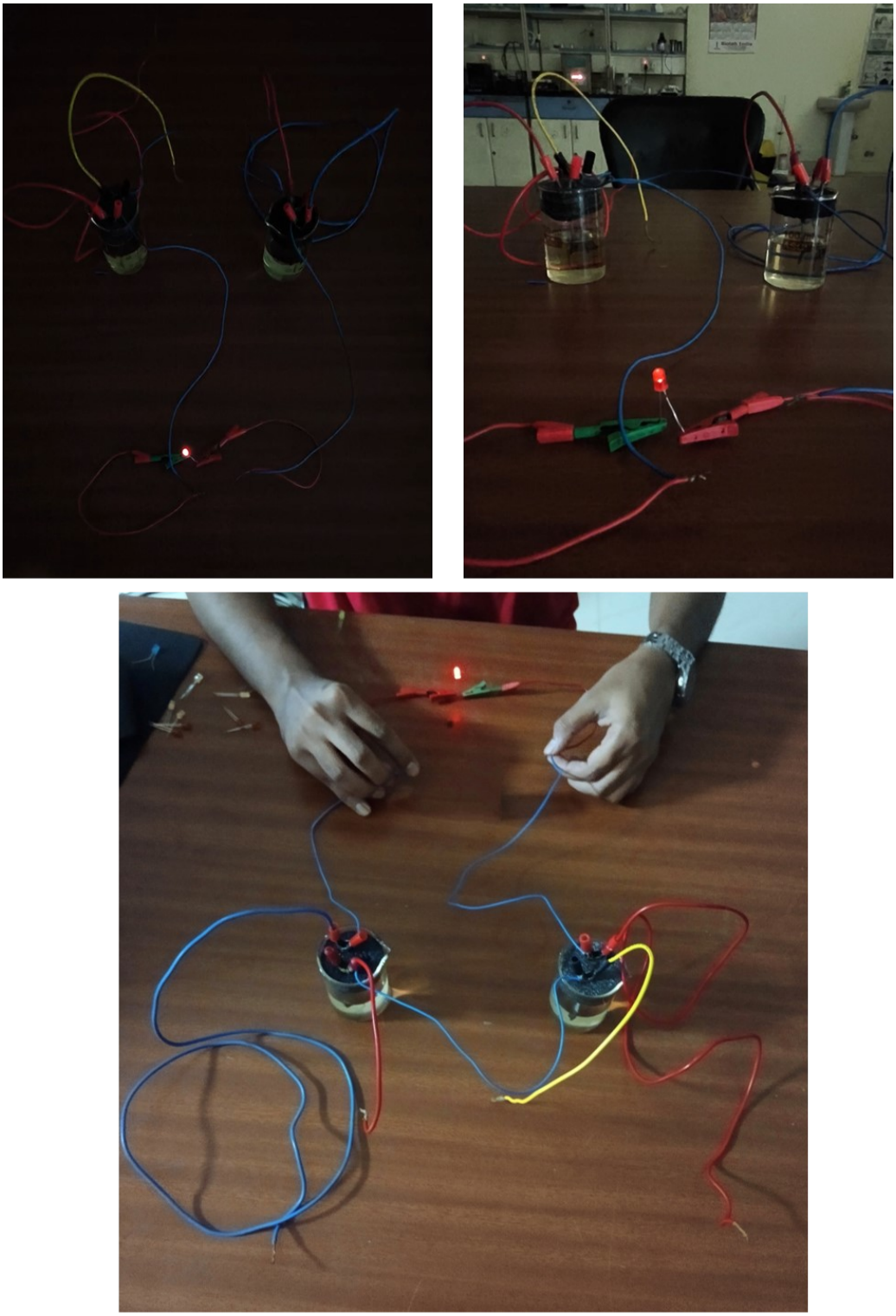

Figure S12: Performance demonstration of the fabricated device in series.

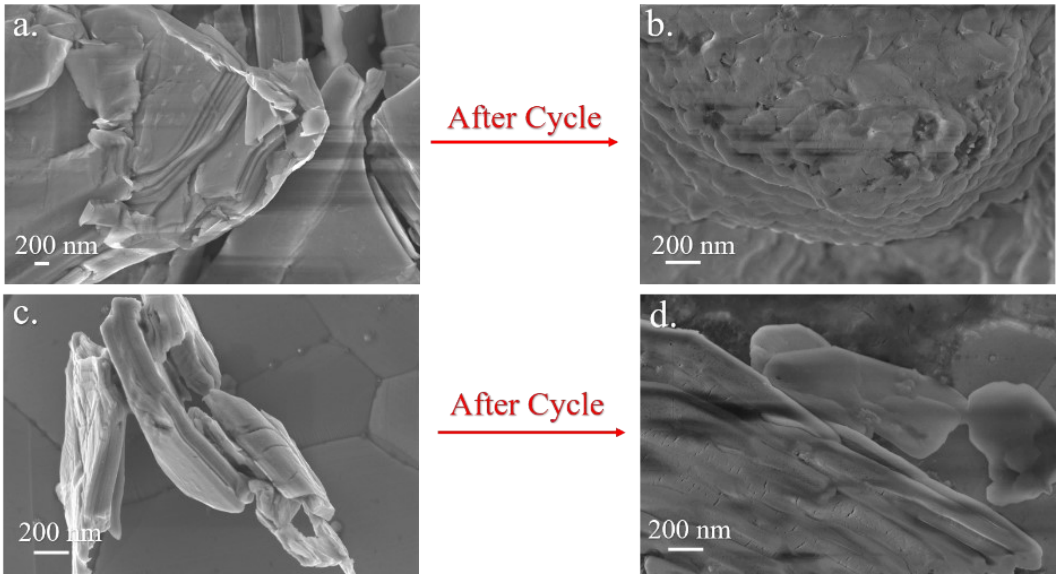

Figure S13: Plan-view FESEM image of pristine (a, b) and irradiated (c, d) $Mo_2TiC_2T_x$ MXene/Ni foam before and after 10,000 cycles.

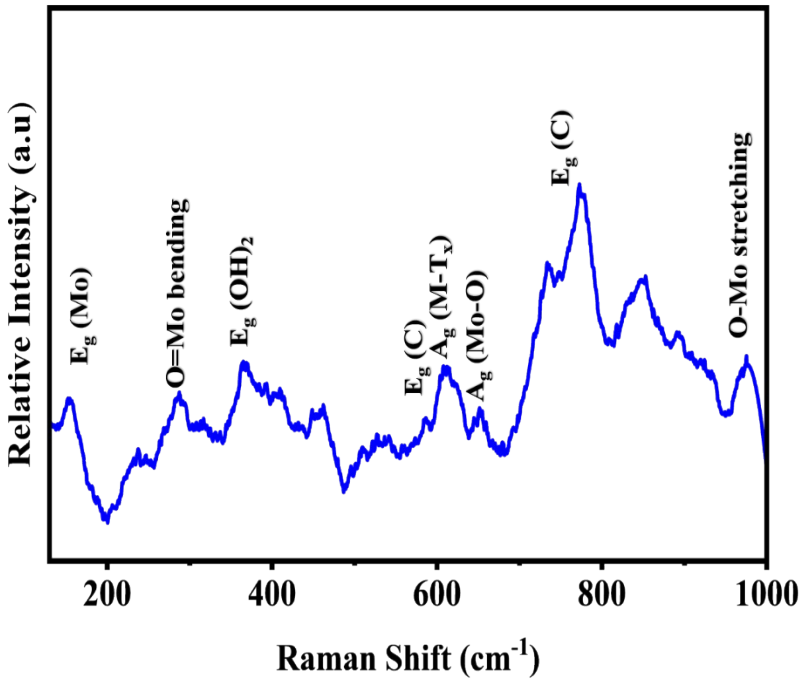

Figure S14: Raman spectra of irradiated $Mo_2TiC_2T_x$ MXene/Ni foam after 10,000 cycles showing phase stability.

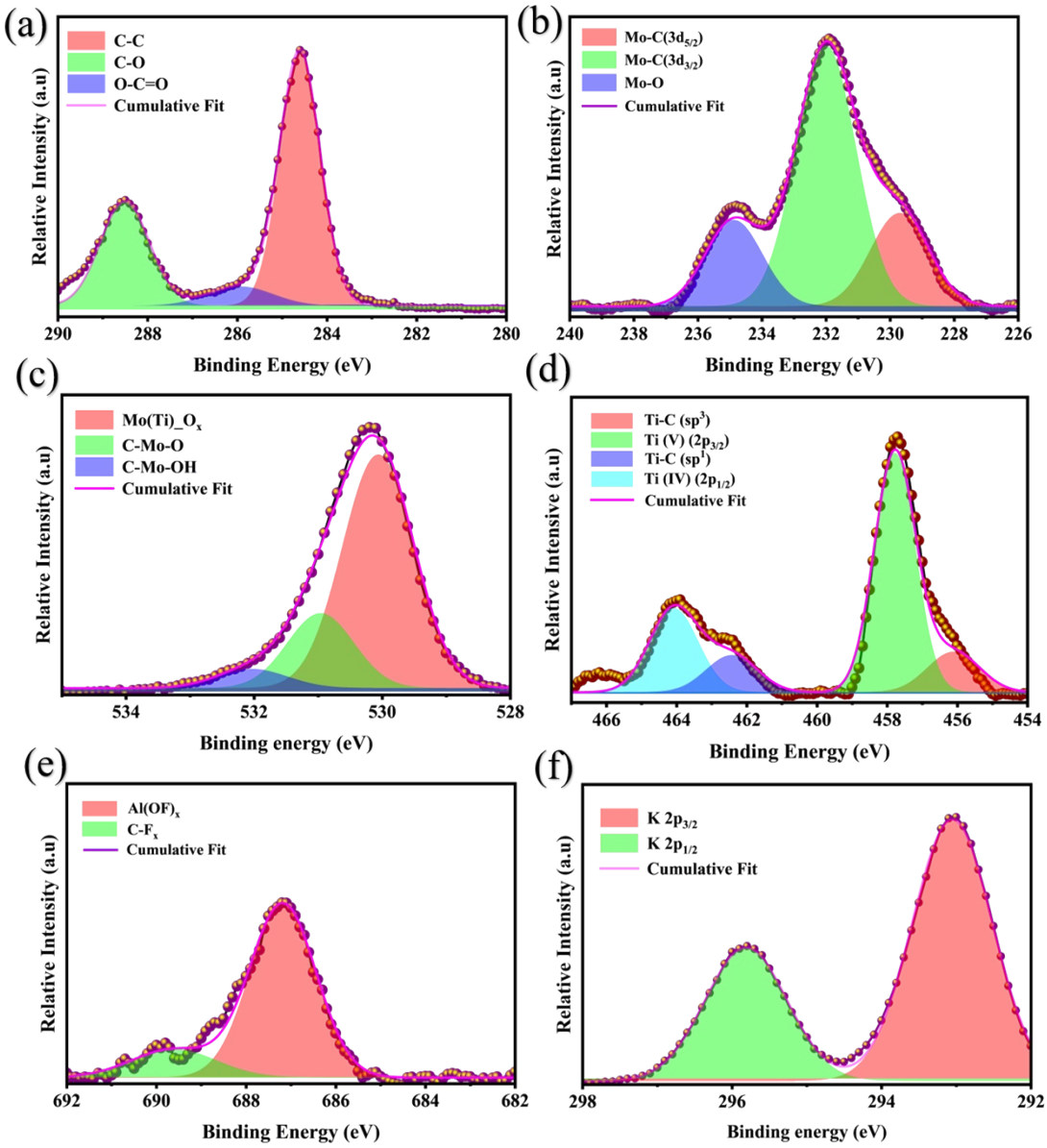

Figure S15: XPS spectra of irradiated $Mo_2TiC_2T_x$ MXene after long charge–discharge cycling, showing binding energies corresponding to (a) C1s (b) Mo 3d, (c) O 1s (d) Ti 2p (e) F 1s (F) K 2p. The presence of K 2p peaks may arise due to defects trap at active sites as well as within the layers, confirming the adsorption/intercalation of K^+ ions.

Table S3:

Comparative Table of $Mo_2TiC_2T_x$ MXene-Based Supercapacitor Electrodes:

Material	Specific Capacitance	Measurement Condition	Electrolyte	Cycling Stability	Reference
Pristine $Mo_2TiC_2T_x$ (multilayer)	96.4 F g^{-1}	1 A g^{-1}	1 M KOH	55% after 10,000 cycles	This work
Ion-beam-irradiated $Mo_2TiC_2T_x$ (this work)	187 F g^{-1}	1 A g^{-1}	1 M KOH	80% after 10,000 cycles	This work
Pristine $Mo_2TiC_2T_x$ (free-standing film)	310 F g^{-1}	5 mV s^{-1}	-	>5,000 cycles	Hakim et al., 2023 [1]
Ni-intercalated $Mo_2TiC_2T_x$ (free-standing film)	682 F g^{-1}	5 mV s^{-1}		>5,000 cycles	Hakim et al., 2023 [1]
Pristine $Mo_2TiC_2T_x$	670 F g^{-1}	2 mV s^{-1}	KOH	-	Ali et al., 2022 [2]
Sn^{2+}-intercalated $Mo_2TiC_2T_x$	670 F g^{-1}	2 mV s^{-1}	KOH	High retention over 10,000 cycles	Ali et al., 2022 [2]
Pristine $Mo_2TiC_2T_x$	425 F g^{-1}	5 mV s^{-1}	1 M KOH	-	Alahmadi et al., 2024 [3]
Delaminated $Mo_2TiC_2T_x$ (free-standing film)	<100 F g^{-1}	2 mV s^{-1}	3 M KOH	-	Bin et al., 2024 [4]

Table S4:

Parameters obtained from the EIS data.

Parameters	Pristine	Irradiated
R_{ct} (Ω)	4.9803	3.1853
R_s (Ω)	0.65867	0.68226
C_1 (F)	7.1543×10^{-3}	7.919×10^{-3}

The following equation used to calculate capacitance from EIS data:

$$\boldsymbol{C}_1 = Q_0^{1/n} \times R_{ct}^{(1-n)/n}$$

where Q_0 and n are constant phase element (CPE) parameters from EIS fit; R_{ct} = charge-transfer resistance (Ω)

References:

[1] M. W. Hakim, S. Fatima, R. Tahir, M. Z. Iqbal, H. Li, S. Rizwan, Ni-intercalated Mo_2TiC_2Tx free-standing MXene for excellent gravimetric capacitance prepared via electrostatic self-assembly, *Journal of Energy Storage* **61** (2023) 106662. https://doi.org/10.1016/j.est.2023.106662

[2] I. Ali, Z. Haider, S. Rizwan, Enhanced pseudocapacitive energy storage and thermal stability of Sn^{2+} ion-intercalated molybdenum titanium carbide (Mo_2TiC_2) MXene, *RSC Advances* **12** (2022) 31923–31934. https://doi.org/10.1039/D2RA05552J

[3] A. N. M. Alahmadi, W. Khalid, M. Saeed, M. I. Masud, S. Karamat, M. Kashif, S. Khan, Pseudocapacitive behavior of 2D molybdenum titanium carbide MXene and polyaniline based nanocomposites electrodes (Enhanced Electrochemical Performance of MWCNT-Assisted Molybdenum–Titanium Carbide MXene as a Potential Electrode Material for Energy Storage Application), *ACS Omega* (2024). https://doi.org/10.1021/acsomega.3c04932

[4] X. Bin, M. Sheng, B. Kong, Y. Luo, J. Xiao, W. Que, The synthesis and supercapacitor application of flexible free-standing Ti_3C_2Tx, Mo_2TiC_2Tx, and V_4C_3Tx MXene films, *Nanoscale* **16** (2024) 15196–15207. https://doi.org/10.1039/D4NR01826E